Proceedings of 2019 IEEE
International Conference on Mechatronics and Automation
August 4 - 7, Tianjin, China

Study on Tracking Stability for a Master-Slave Vascular Interventional Robotic System

Jian Guo[1], Lei Qi[1] and Shuxiang Guo[1,2,*]

[1]*Tianjin Key Laboratory for Control Theory & Application in Complicated Systems and Biomedical Robot Laboratory*
Tianjin University of Technology
Binshui Xidao 391, Tianjin, China
jianguo@tjut.edu.cn;
1576705909@qq.com

Cheng Meng[1] and Qi Zhan[1]

[2]*Intelligent Mechanical Systems Engineering Department*
Faculty of Engineering
Kagawa University
Takamatsu, Kagawa, Japan
*corresponding author: guo@eng.kagawa-u.ac.jp

***Abstract* - In this paper, in order to solve the problem of tracking stability of a master–slave vascular interventional robotic system, the related research was made. A conditioning circuit and a filtering algorithm were designed to suppress the problem of the jitter from the slave of the robot. The master-slave tracking system uses differential control, and the stability of the input signal directly affects the stability of the differential control. In order to obtain a stable and accurate master-slave axial displacement signal, a linear attenuation circuit with filter follow-up function is designed as the acquisition and conditioning circuit, and the collected information is Kalman filtered to obtain a stable and accurate axis displacement signal. The axial displacement signal acts as the input to the master-slave tracking system, and the stability of the input enhances the stability of the differential control. The experimental results showed that the linear attenuation filter follower circuit and Kalman filter can effectively enhance the stability of the acquired signal, which enhances the motion stability of the master-slave tracking system with differential control and the problem of dither from the slave manipulator during the motion is solved.**

Index Terms* -*Vascular interventional robot, Stability of the master-slave tracking, Linear attenuation tracking filter circuit, Kalman filter

I. INTRODUCTION

In recent years, many countries have begun to pay more attention to cardiovascular and cerebrovascular diseases [1]. Cardiovascular and cerebrovascular diseases are usually treated in two ways, one is traditional open surgery and the other is catheterization. Among them, open surgery is performed at the location of the lesion. The surgical procedure is very damaging to the patient. The patient needs to bear a lot of pain and the risk of surgery is high [2]. The catheter intervention is guided by medical imaging. Special medical catheters and guide wires are introduced into the blood vessels to treat the lesions in the blood vessels accordingly. The incisions are only the size of rice grains [3].

The development of robotics in the medical field has also made a major breakthrough, and medical robots have emerged [4]. The vascular interventional robot can not only assist the doctor to complete complicated surgical operations, but also reduce human error during the operation to improve the safety and stability of the operation, protect the doctor from X-ray damage, and the robot operation ratio Manual operation is more stable [5-6].

Motion scaling based master-slave control is proposed by Zhenqiu Feng et al for different stages of the vascular interventional robot delivery to improve the safety of surgery [7]. Laura Cercenelli et al developed a highly compact and versatile remote catheter navigation system named CathROB which has the inherently safe design and the automatic navigation functionalities [8-9]. HJ Cha et al designed a catheter intervention system to treat ablation of the heart. The system has three degrees of freedom: axial, radial and rolling, which can change the size of the operating force by changing the current in the motor [10].

The master-slave tracking synchronization accuracy problem is an important issue in the study of vascular interventional surgery robots, and the stability of displacement acquisition information is the premise of master-slave tracking synchronization accuracy.

II. OVERVIEW OF THE MASTER–SLAVE VASCULAR INTERVENTIONAL ROBOTIC SYSTEM

The vascular interventional surgery robot we designed is a master-slave teleoperation system. A device for cooperative operation of a catheter and a guide wire in a vascular interventional procedure, the device being divided into a master-side and a slave slave, chara`cterized in that it can simultaneously control the catheter and the guide wire and perform cooperative operation. The master-side portion includes a master operator, a force feedback damper, a master

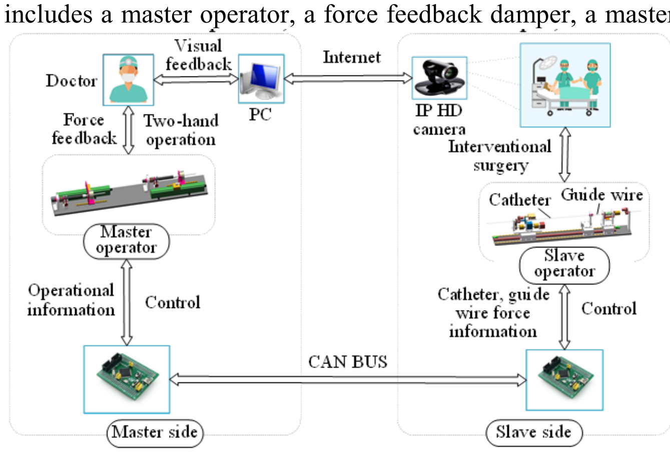

Fig. 1 Schematic diagram of the master-slave teleoperation system

controller and a PC display screen, wherein the master operator is divided into a catheter operating device and a guide wire operating device; theslave slave portion includes an IP camera, a slave operator, and a slave controller, catheter and guide wire. The operation flow is as follows: the doctor uses both hands to separately control the catheter operating device and the guide wire operating device of the master operator, and the master controller collects the operation information of the doctor, including axial displacement information and radial rotational displacement information, and then the master controller passes the information [11]. *CAN* communication is transmitted to the slave controller; from the input slave of the controller, the doctor operation information transmitted by the master controller and the force information of the catheter and the guide wire collected from the sensor on the operator are received, and then the output terminal is connected to the master controller, The force information is transmitted to the master controller through the *CAN* bus; the master controller controls the master operator force feedback damper to feed the force back to the doctor [10]; the IP high-definition camera collects the real-time motion image of the scene from the operator, and the output slave and the master-side PC The display is connected via the Internet and the doctor can watch it on the display of the master PC. The display can also display information about the movement of the catheter and guidewire as well as the force information, providing visual feedback to the doctor. The schematic diagram of the master-slave teleoperation system is shown in Fig. 1.

The paper introduce es a master-slave minimally invasive vascular interventional robot that meets the doctor's operating habits and can realize the coordinated operation of the catheter and guide wire. It can realize the coordinated intervention of the catheter and the guide wire, and enables the doctor to go like a traditional operation. Operation, in line with the doctor's operating habits, can also directly feedback the real-time force and visual information to the doctor, increase the doctor's sense of presence during surgery, improve the safety and operability of the interventional surgery, and the structure is simple and easy to implement. The mechanical structure of the master-slave manipulator is shown in Fig. 2.

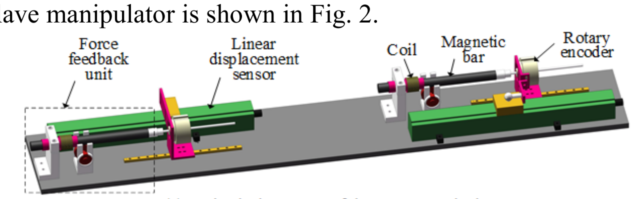

(a)Mechanical structure of the master manipulator

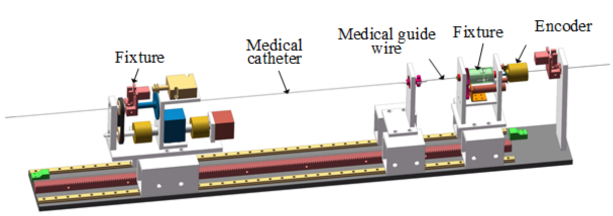

(b)Mechanical structure of the slave manipulator

Fig. 2 Mechanical structure of the master-slave manipulators

III Stability Tracking Control Based On Filtering Algorithm

A. Design of linear attenuation filter circuit

This design uses the linear displacement sensor of the non-contact magnetostrictive measurement principle to detect the axial displacement of the master operator. The sensor uses NOVOSTRICTIVE measurement technology to directly, accurately and absolutely reflect the linear displacement. Sensor measurement is achieved by using a floating magnetic block non-contact method, so the sensor has no mechanical wear, and the output signal is 0.1-10 VDC (load ⩾ 5kΩ) corresponding to a working range of 200 mm.

Since the voltage acquisition range of the single-chip ADC used is 0-3.3V, it is necessary to linearly attenuate the sensor output voltage signal. The linear attenuation of the signal can be simply processed by the principle of resistor divider. However, the simple use of resistor divider may cause impedance mismatch or output voltage fluctuation. The circuit in this paper is based on resistor divider, second-order passive low-pass filter , and voltage follow-up. The signal attenuation circuit designed by the principle of the device can realize the linear attenuation, filtering and load-increasing function of the signal. As the pre-stage circuit of the single-chip *ADC* acquisition circuit, the usability and stability of the collected information are effectively improved. The circuit diagram of linear attenuation filter follower is shown in Fig. 3.

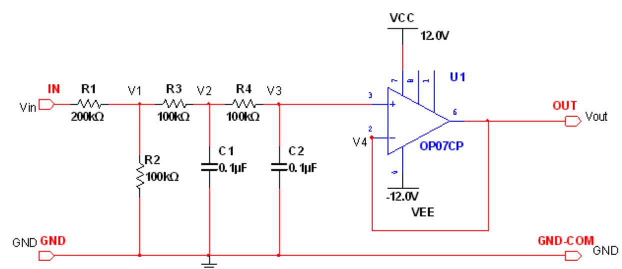

Fig. 3 Circuit diagram of linear attenuation filter follower

1) Design of voltage divider circuit

In Fig. 3, *R1* and *R2* divide the voltage of Vin to linearly attenuate the output voltage to meet the *ADC* voltage acquisition range of the microcontroller. The relationship between Vin and V1 is as follows:

$$V1 = \frac{R2}{R1+R2} Vin \tag{1}$$

$$V1 = \frac{100K}{200K+100K} Vin = \frac{1}{3} Vin \tag{2}$$

When $Vin = 10V$:

$$V1 = \frac{1}{3} \times 10V \approx 3.3V \tag{3}$$

It can be obtained from (1), (2) and (3). The sensor voltage output 0-10V can be linearly converted to 0-3.3V, thus satisfying the *ADC* voltage acquisition range of the single chip microcomputer.

2) Design of second-order passive low-pass filter circuit

In Fig. 4, resistor *R3*, capacitor *C1*, resistor *R4*, and resistor *C2* together form a second-order passive low-pass filter. A filter is an electronic device that can pass a useful frequency signal while suppressing or greatly attenuating the unwanted frequency signal. Usually, the signal frequency range that can pass is defined as a pass band, and the blocked or attenuated signal frequency range is called a resistance. The boundary frequency of the band, pass band and stop band is called the cutoff frequency. The ideal filter circuit should have a zero-attenuation amplitude-frequency response and a linear phase response in the passband, and should have an infinite amplitude attenuation in the stopband. In this paper, the low-pass filter circuit is used to filter *V1*. The schematic diagram of amplitude-frequency response curve of low-pass filtering is shown in Fig. 4.

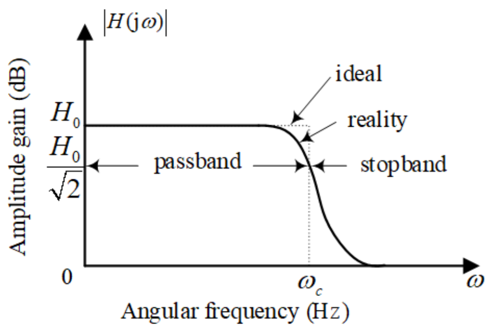

Fig. 4 Schematic diagram of amplitude-frequency response curve of low-pass filtering

In Fig. 4, H_0 represents the amplitude of the low frequency gain $|H(j\omega)|$. It can be seen from the figure that its function is to completely attenuate all frequencies greater than ω_c by a low-frequency signal from zero to a certain cut-off angle frequency ω_c, so its bandwidth $B=\omega_c$, second-order passive low-pass filter in multi-frequency, the frequency response analysis in the domaster is as follows.

In Fig. 3, $V_1(j\omega)$ is used as the excitation signal of the second-order filtering, and $V_3(j\omega)$ is the response signal of the second-order filtering, where $R_3=R_4=R$, $C_1=C_2=C$.

Then the gain of the filter in the passband is:

$$K=\frac{V_3}{V_1}=1 \tag{4}$$

The transfer function in the complex frequency domaster is:

$$H(j\omega)=\frac{V_3(j\omega)}{V_1(j\omega)}=\frac{1}{1-\omega^2R^2C^2+j3\omega RC}=|H(j\omega)|\angle\theta(\omega) \tag{5}$$

The amplitude-frequency characteristic equation is:

$$|H(j\omega)|=\frac{1}{\sqrt{(1-\omega^2R^2C^2)^2+9\omega^2R^2C^2}} \tag{6}$$

$|H(j\omega)|$ is the amplitude gain in (6).

The phase frequency characteristic equation is:

$$\theta(\omega)=-\arctan\left(\frac{3\omega RC}{1-\omega^2R^2C^2}\right) \tag{7}$$

If the gain of the filter in the passband is K, the corresponding frequency is called the cutoff frequency ω_c when its gain drops to $K/\sqrt{2}$, that is, the gain is reduced by $3dB$.

From

$$20\lg\left|\frac{|H(j\omega)|}{K}\right|=20\lg\left|\frac{1}{\sqrt{(1-\omega^2R^2C^2)^2+9\omega^2R^2C^2}}\right|=-3 \tag{8}$$

$$\text{Got: } \omega_c=37.40 \tag{9}$$

Then the cutoff angle frequency:

$$\omega_c=\frac{1}{2.6724RC}=\frac{0.3742}{\tau} \tag{10}$$

$$\text{Where: } \tau=\frac{1}{RC} \tag{11}$$

The cutoff frequency is:

$$f_c=\frac{\omega_c}{2\pi} \tag{12}$$

When R = 100K and C = 0.1μF, f_c=5.96 is obtained from (10), (11), and (12). Simulation by Multisim, as shown in Fig. 5, The filter amplitude-frequency characteristic curve (a) and the phase-frequency characteristic curve (b) are obtained as shown in Fig. 6.

As shown in Fig. 6, it can be seen from Fig. 6 (a) that the cutoff frequency at -3*dB* is 5.953*Hz,* and the frequency higher than 5.953*Hz* can be effectively filtered out, resulting in a more stable output *DC* voltage signal, thus meeting the stability requirements of this paper. It can be seen in Fig. 6 (b) that the corresponding phase angle at the cutoff frequency ω_c is -52.529°.

3) Design of voltage follower

A voltage follower is a type of electronic component that implements a change in the output voltage following the input voltage. That is, the voltage amplification of the voltage follower is always less than and close to one. The high input impedance of the voltage follower and the low output work better and it also has the function of buffering, isolating and improving the load capacity [12]. The role. It can be stage;

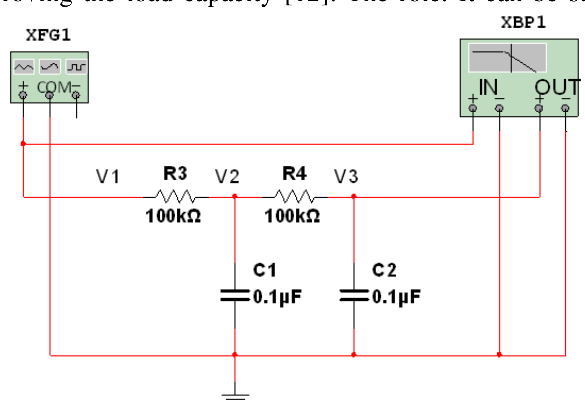

Fig. 5 The circuit diagram of second order RC low-pass filter

when the output impedance is very low, the circuit of the latter stage is equivalent to a constant voltage source, that is, the output voltage is not affected by the impedance of the subsequent stage circuit. influences. A circuit that is equivalent to an open circuit to the pre-stage circuit and whose output to an open circuit to the pre-stage circuit and whose output voltage is not affected by the impedance of the latter stage is of course isolated, so that the circuits of the front and rear stages do not affect each other. Another advantage of applying the voltage follower is that the input is improved. Impedance, in this way, the capacity of the input capacitor can be greatly reduced, providing a prerequisite for the application of high-quality capacitors.

As shown in Fig. 3, the voltage follower is composed of OP07CP integrated op amp. OP07 is a low noise, high open loop gain, non-chopper-stabilized bipolar op amp IC. By using the linear attenuation filter follower circuit as the pre-stage circuit collected by the single-chip *ADC*. The schematic diagram of linear filter follower circuit as pre-stage circuit acquisition is shown in Fig. 7.

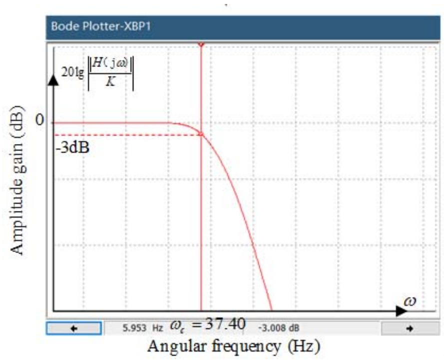

(a)Filter amplitude frequency characteristic curve

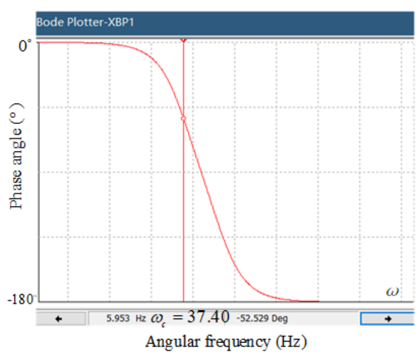

(b)Filter phase frequency characteristic curve

Fig. 6 Simulation of the amplitude and frequency characteristics of the filter amplitude

B. *Kalman Filtering Algorithm*

The stability and accuracy of the axial displacement information output by the master linear displacement sensor collected by the single-chip microcomputer is an important problem of accurate and stable follow-up of the axial displacement of the master and secondary slaves. In this paper, the Kalman filter algorithm is used to process the axial displacement information collected by the *ADC* to reduce the error and noise, thus enhancing the accuracy and stability.

1) The concept of Kalman Filter

Kalman filter is R. E. An iterative algorithm applied to discrete linear filtering from Kalman's 1960 estimate of system state from noise-containing measurements [13]. Since its solution is calculated by recursion, Kalman filtering is also a real-time recursive algorithm that can be implemented by a computer. The filtering process is divided into two parts: state update and measurement update. Firstly, the system of the next state is estimated according to the current system state and noise variance by the state update equation [14]. Then, the measurement update equation is used to add the observation of the system as the input of the filter. In the a priori estimation state obtained by the state update equation, the posterior estimation of the system state is obtained, and the optimal system state is estimated by continuously performing the variance recursion.

2) Design of Kalman filter

The operation of the Kalman filter masterly consists of two phases, estimation and update [15]. In the estimation phase, the filter estimates the current time state according to the state of the previous time; in the update phase, the filter optimizes the system prediction value obtained in the estimation phase by using the current time observation value to obtain a more accurate new estimation value. The specific implementation process is as follows.

Prior state prediction equation:

$$\hat{X}_{(k|k\text{-}1)} = F\hat{X}_{(k-1|k-1)} + Bu_{(k-1)} \tag{13}$$

In (13), $\hat{X}_{(k|k-1)}$ is system prediction value at time *k*, and $\hat{X}_{(k-1|k-1)}$ is the estimated value at time *k-1*, *F* For the state transition matrix, *B* is the control matrix, and $u_{(k-1)}$ is the system control, which uses the state of the previous moment to estimate the current state.

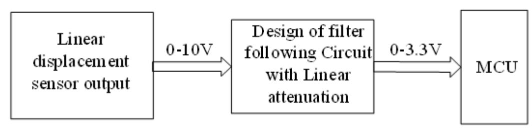

Fig. 7 Schematic diagram of linear filter follower circuit as pre-stage circuit acquisition

Prior state prediction error covariance transfer equation:

$$P_{(k|k\text{-}1)} = FP_{(k-1|k-1)}F^T + Q \tag{14}$$

In (14), $P_{(k|k-1)}$ is the a priori prediction error covariance matrix at time *k*; $P_{(k-1|k-1)}$ is the posterior state at time *k-1* The prediction error covariance matrix reflects the accuracy of the previous state estimation, and *Q* is the system noise covariance matrix.

Observation equation:

$$Z_k = HX_k + v \tag{15}$$

In (15), Z_k is the observation matrix at time *k*, *H* is the observation transformation matrix, and *v* is the observation noise at time *k*.

Kalman gain equation:

$$K_k = \frac{P_{(k|k\text{-}1)}H^T}{(HP_{(k|k\text{-}1)}H^T + R)} \tag{16}$$

In (16), *R* is the covariance matrix of the observed noise, and K_k is the Kalman gain at time *k*.

Posterior state prediction equation:

$$\hat{X}_{(k|k)} = \hat{X}_{(k|k\text{-}1)} + K_k(Z_k - \mathrm{H}\,\hat{X}_{(k|k\text{-}1)}) \tag{17}$$

In (17), the predicted value is adjusted using the dynamic change of the Kalman gain K_k.

Posterior state prediction error covariance equation:

$$P_{(k|k)} = (I\text{-}K_kH)\ P_{(k|k-1)} \tag{18}$$

In (18), I is an identity matrix, and the update of the Kalman gain K_k. is achieved by updating $P_{(k|k)}$.

In this paper, only the Kalman filter is applied to the voltage value of the linear displacement sensor collected by the *ADC*[16]. The observed variable selects the *ADC* acquisition value, so the state variable is selected as the scalar, where $F=1, B=1, H=1, u_{(k-1)}=0$.

Then the above formula is simplified:

$$\hat{x}_{(k|k-1)} = \hat{x}_{(k-1|k-1)} \tag{19}$$

$$p_{(k|k-1)} = p_{(k-1|k-1)} + q \tag{20}$$

$$z_k = x_k + v \tag{20}$$

$$k_k = \frac{p_{(k|k-1)}}{(p_{(k|k-1)} + r)} \tag{22}$$

$$\hat{x}_{(k|k)} = \hat{x}_{(k|k-1)} + k_k(z_k - \hat{x}_{(k|k-1)}) \tag{23}$$

$$p_{(k|k)} = (1-k_k)\, p_{(k|k-1)} \tag{24}$$

The above parameters are all scalar, which is convenient for implementing the algorithm in *C* language by *C* language, which reduces the programming complexity of the algorithm. The actual measured Kalman filter *C* program has an execution event of no more than 10μs, which ensures the real-time measurement. The size of q and r determines the effect of the Kal filter on the filtering of the collected information. After simulation and analysis, this paper uses q=1.0e-8 and r=1.1171e-06.

IV Experimental Design And Analysis

A. *Experimental design*

In this paper, a more stable acquisition of the master line linear displacement sensor output analog voltage, a linear attenuation filter follower circuit is designed as the pre-stage circuit of the single-chip *ADC* acquisition, and the Kalman filter algorithm is used again to denoise the acquisition voltage of the single-chip *ADC*. The result is a more stable voltage signal. Compared with the simple resistor divider circuit, the linear attenuation filter follower circuit can output a more stable voltage signal, and the Kalman filter algorithm can further remove the signal of the collected voltage to obtain a more stable voltage signal. The experiment is masterly divided into displacement sensor remasters unchanged during data recording; In the second step, the position of the sliding magnetic block is three steps. The first step is to use the *NI USB-6210* acquisition card to collect the analog voltage value output by the linear displacement sensor after simple series resistance partial voltage. The position of the sliding magnetic block of the linear kept unchanged, and the analog voltage outputted by the linear attenuation filter following circuit is collected by the acquisition card[17], and the position of the sliding magnetic block is kept unchanged during the same acquisition process; the third step is to perform Kalman filtering programming with matlb. Simulation, which uses the principle mentioned in Section 3.2 to carry out Kalman algorithm programming, the data uses the voltage value collected in the second step, and finally draws the three graphs with matlab for comparison. The schematic diagram of the experimental process is shown in Fig. 8.

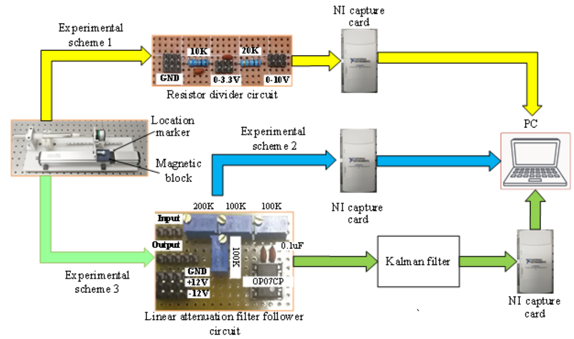

Fig. 8 Schematic diagram of the experimental process

B. *Experimental results*

Through the above experimental flow, three sets of data, a set of data obtained by simple resistor divider, the second set is the data obtained by the linear attenuation filter follower circuit, and the third set is obtained by the Kalman filter of the second set of data. Data, then a comparison graph of three sets of data is drawn by matlab, as shown in Fig. 9.

C. *Experimental analysis*

In Fig. 9, the blue line is the data obtained by the resistor divider, the red line is the data obtained by the linear attenuation filter circuit, and the yellow line is the Kalman filter to obtain the data. It can be seen from the figure that using only the resistor divider to achieve linear attenuation of the signal will generate some noise[18-19], making the output voltage unstable, and the stability and accuracy of the vascular interventional surgery robot is a great influencing factor, so the data is made . It is very important to become more stable and accurate; the red line is the voltage output obtained by the linear attenuation filter follower circuit designed in this paper. It can be seen that this circuit can effectively suppress the noise and make the data more stable and accurate; The data is stable and accurate. In this paper, the Kalman filter processing is performed on the data obtained by the linear attenuation filter follower circuit, and finally the more stable data is obtained, which has an important influence on the stability and control of the platform.

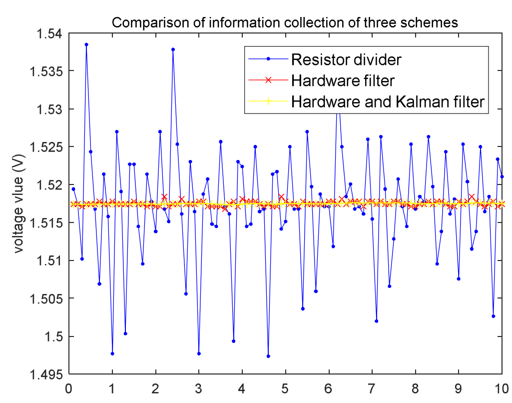

Fig. 9 Experimental comparison Curve of three schemes

Because the master-slave tracking system designed in this paper adopts the difference control, the difference between the input and feedback values is used to control the start and stop of the system motion, and the stability of the input directly affects the stability of the difference. When the difference is close to zero, if the input is fluctuating, the difference will be close to the fluctuation of zero small range, and the larger the input fluctuation, the larger the fluctuation of the difference, which will cause the slave robot to shake when it stops. In this paper, the conditioning circuit and the filtering algorithm effectively suppress the fluctuation of the input signal, thus effectively suppressing the jitter problem of the slave manipulator.

V CONCLUSIONS

In this paper, the motion stability of the master-slave tracking system of the vascular intervention robot was effectively improved, and the jitter problem of the slave manipulator in the process of motion was effectively suppressed. Compared with the traditional resistance voltage divider circuit, it was verified that the linear attenuation circuit with filtering and tracking function can better enhance the stability of slave motion. At the same time, it was verified that Kalman filter can make the slave stable motion more than the first two schemes. The result showed that the stability of the motion process was effectively enhanced.

ACKNOWLEDGMENT

This research is supported by National Natural Science Foundation of China (61703305); Key Research Program of the Natural Science Foundation of Tianjin (18JCZDJC38500) and Innovative Cooperation Project of Tianjin Scientific and Technological Support (18PTZWHZ00090).

REFERENCES

[1] X. Bao, S. Guo, N. Xiao, Y. Li, C. Yang and Y. Jiang, "A cooperation of catheters and guidewires-based novel remote-controlled vascular interventional robot," *Biomedical Microdevices*, vol. 20, no. 1, pp.20, 2018.

[2] J. Guo, S. Guo, L. Shao, P. Wang, and Q. Gao, "Design and performance evaluation of a novel robotic catheter system for vascular interventional surgery," *Microsystem Technologies*, vol. 22, no. 9, pp. 2167-2176, 2015.

[3] H. Su, W. Shang, G. Li, N. Patel and G. Fischer, "An MRI-Guided Telesurgery System Using a Fabry-Perot Interferometry Force Sensor and a Pneumatic Haptic Device," *Annals of Biomedical Engineering*, vol. 45, No. 8, pp. 1917-1928, 2017.

[4] C. He, S. Wang and S. Zuo, "A linear stepping slaveovascular intervention robot with variable stiffness and force sensing," *International Journal of Computer Assisted Radiology and Surgery*, vol. 13, no. 5, pp. 671-682, 2018.

[5] L. Cercenelli, B. Bortolani and E. Marcelli, "CathROB: A Highly Compact and Versatile Remote Catheter Navigation System," *Applied Bionics and Biomechanics*, vol. 2017, no. 8, pp. 1-13, 2017.

[6] Y. Thakur, D. Holdsworth and M. Drangova, "Characterization of catheter dynamics during percutaneous transluminal catheter procedures," *IEEE Trans Biomed Eng*, vol. 56, no. 8, pp. 2140-2143.

[7] J. Cheng, "Research on structural nonlinear behavior recognition based on Kalman filtering and partial observation," Hunan University, 2018.

[8] M. Gao, Y. Yang, L. Kong, "Design of low-pass filter for second-order voltage-controlled voltage source," Electronic Technology, vol. 47, no. 3, pp.73-75, 2010.

[9] L. Jones, "Human and Machine Haptics," By M. Cutkosky, R. Howe, K. Salisbury, and M. Srinivasan, Eds., MIT Press, 2000.

[10]Z. Feng, G. Bian, X. Xie, Z. Hou and J. Hao, "Design and evaluation of a bioinspired robotic hand for percutaneous coronary intervention," *Proceedings of 2015 IEEE International Conference on Robotics and Automation*, pp. 5338-5343, 2015.

[11]S. Guo, J. Guo, L. Shao, P. Wang, and Y. Wang, "Performance evaluation of the novel grasper for a robotic catheter navigation system," *Proceedings of 2014 IEEE International Conference on Information and Automation*, 2014.

[12]H.J. Cha, B.J. Yi and J.Y. Won, "An assembly-type master-slave catheter and guidewire driving system for vascular intervention," *Proc Inst Mech Eng H*, vol. 231, no. 1, pp. 69-79, 2017.

[13] W. Shang, H. Su, G. Li,and GS. Fischer, "Teleoperation System with Hybrid Pneumatic Piezoelectric Actuation for MRI-Guided Needle Insertion with Haptic Feedback", *IEEE/RSJ International Conference on Intelligent Robots & Systems Rep US, 2013.*

[14]M. Hong, "Research on speech signal denoising algorithm based on wavelet transform," Nanjing University of Posts and Telecommunications, 2018.

[15]Z. Xu, "Research on speed measurement method of incremental photoelectric encoder based on Kalman filter". University of Science and Technology of China, 2018.

[16]Y. Zhao, S. Guo, Y. Wang, J. Cui, Y. Ma, Y. Zeng, X. Liu, Y. Jiang, Y. Li, L. Shi, N. Xiao, "A CNNs-based Prototype Method of Unstructured Surgical State Perception and Navigation for an Slaveovascular Surgery Robot", Medical & Biological Engineering & Computing, in press, 2019.

[17]S. Guo, Y. Song, X. Yin, L. Zhang, T. Tamiya, H. Hirata, H. Ishihara, "A Novel Robot-Assisted Slaveovascular Catheterization System with Haptic Force Feedback", The IEEE Transactions on Robotics, 2019.

[18]X. Bao, S. Guo, N. Xiao, L. Shi, "Design and Evaluation of Sensorized Robot for Minimally Vascular Interventional Surgery", Microsystem Technologies, 2019.

[19]J. Guo, S. Guo, "A Marker-based Contactless Catheter-sensing Method to Detect Surgeons' Operations for Catheterization Training Systems", Biomedical Microdevices, Vol.20, No.3, 2018.